



Novel Method for Wind Turbines Blades Damage Classification using Image Processing

M A Garduño-Ramón, E Resendiz-Ochoa, L A Morales-Hernandez, and R A Osornio-Rios*

HSPdigital – CA Mecatronica, Facultad de Ingenieria Campus San Juan del Rio, Universidad Autonoma de Queretaro, Rio Moctezuma 249, 76807 San Juan del Rio, Queretaro, Mexico

Received 05 April 2018; revised 27 November 2020; accepted 03 December 2020

Wind turbine generators are spreading around the world due to its advantages over fossil fuels. Structural monitoring of them is important to increase operation and reduce maintenance times. Visual inspection is highly influenced by the human factor due to the working conditions. Image processing supported by vision systems offers high advantages reducing times, being the software and processing algorithms, which generates added value. In this paper, a novel method for wind turbines blades damages analysis is presented using image processing and a classifier based on dimensional features. The image acquisition is performed using a reflex camera with a telephoto and geo-location enabled. The faults analyzed include cracks, edge erosion, and electric discharge.

Keywords: Crack, Dimensional features, Generators, HAWT, Edge erosion

Introduction

The wind as a way to obtain clean energy has proven to be a highly reliable option and an alternative to fossil fuels.¹ Its popularity has spread throughout the world and until 2015 it has been reported that the installed capacity reaches 433 GW²; even some countries, such as Denmark, are close to reaching 50% of their energy production based on wind energy.³ The power generation process is usually carried out by using horizontal axis wind turbines (HAWT) over which an air flow passes through; this kinetic energy rotates the blades of the wind turbine, and is then transformed into electrical energy; finally, it is stored or distributed as required.⁴ Factors such as operation and maintenance (O&M), within the structural health monitoring (SHM) of wind turbines, directly affect the leveled cost of energy (LCOE).⁵ For wind turbine blades the main downtimes can be associated to rotor imbalances, rear edge disjunctions, cracks (transverse and longitudinal) and erosion at the leading edge, edge vibration, lightning, and icing.⁶

Traditional monitoring systems require contact type sensor arrays that involve instrumentation, maintenance and cost problems^{7,8}, as well as ineffectiveness in locating the fault or that are simply

impractical to implement in service.⁹ Blade inspection is usually done using ground-mounted telescopes, however, the use of digital camera images has gained relevance in recent years. Thermographic images have been used to identify damage to blades in wind turbines during operation and on land by means of inducing heat¹⁰; in the same way, infrared images taken at night during the operation of the wind turbine allow detecting the presence of defects, damages or ice due to the heat change of the affected area.^{11,12} Aerial photography using unmanned aerial vehicles (UAV), meanwhile, means a revolution in the way wind turbines are monitored and inspected, allowing to use any kind of range camera sensor to inspect the blades.¹³ In general, one can say that the software behind the image processing system, as well as the user's interpretation experience, is what generates added value but also generates uncertainty. The digital processing of images offers a great alternative to use for complex and repetitive tasks or that imply a human factor that compromises them. In the state of the art methodologies have been proposed for the analysis and automatic detection of faults in motors or in electrical circuits using thermographic sensors¹⁴; in other areas, such as medical, digital image processing helps in the detection and diagnosis of certain problems and diseases like breast cancer and melanoma¹⁵; in all of these applications, the advantages offered by simplifying processes, reducing

*Author for Correspondence
E-mail: raosornio@hspdigital.org

time and, above all, providing support to the system operator are highlighted so that they can assist in the information provided by these systems and proceed to take decisions. Many of these systems are assisted by automatic segmentation methods, which offer one of the best alternatives to quickly and directly process the images obtained in the different processes measured.^{16,17} The images offer a large amount of information that properly classified allows to detect objects, colors, shapes, and trends. Automatic image classifiers are based on learning the essential characteristics of a specific problem and answering the belonging to a specific class. These classifiers can be as simple as a decision tree or as complex as a neural network, in both cases managing to deliver adequate results. In summary, there is a need for inspection techniques of wind turbine blades based on digital image processing that can classify and quantify damages in wind turbine blades automatically.

This paper presents a novel methodology based on image processing and classification of characteristics that help in the task of detection and classification of three type of failures commonly found in wind turbine blades. The methodology uses contour detectors, as well as automatic thresholding methods supported by the proposal of a classification system that considers spatial aspects of the image and the segmented regions to determine if the fault corresponds to a problem of crack, electric shock or wear at the edge of the blade automatically, so that it serves as an auxiliary and base for a future development that considers more types of failures. The system uses geo-localized images acquired by means of a reflex camera with a telephoto lens on the ground level so that the system reduces inspection times. The methodology was tested using synthetic and real images with good results.

Thresholding

A threshold is a segmentation tool that tries to separate the background from the object. It operates from the establishment of a threshold value, T , defined by the user and then two regions are obtained, one higher or equal that T and one lower. Since the characteristics of the image are always different, in practice semi-automatic or automatic thresholding algorithms are a better option. Otsu's method is a powerful and popular segmentation tool based on the image histogram which selects the optimal threshold value (t^*) maximizing the between-class variance (σ_B^2) as depicted in Eq. (1).

$$t^* = \arg \max_{0 \leq t \leq L} \sigma_B^2 \quad \dots (1)$$

where L denotes the total of grayscale values in the image. The between-class variance (σ_B^2) is determined as shown in Eq. (2).

$$\sigma_B^2 = w_1(t)(\mu_1(t) - \mu_T)^2 + w_2(t)(\mu_2(t) - \mu_T)^2 \quad \dots (2)$$

The probabilities of the two separated classes separate by the threshold (t) are denoted by w_1 and w_2 , meanwhile, μ_1 and μ_2 are the mean gray values of the classes.¹⁸ The threshold algorithm proposed by Hamadani employs statistics from the image like mean, μ , and standard deviation, σ , to perform the image segmentation.¹⁹ The threshold value calculation is shown in Eq. (3).

$$T = k_1 \times \mu + k_2 \times \sigma \quad \dots (3)$$

Both k_1 and k_2 are established manually by the user or by some supervised method, specifically for this paper $k_1 = 0.9$ and $k_2 = 0.1$. The mean (μ) calculation of an image $f(i, j)$ of size $M \times N$ is equal to $\mu = (1/(M \times N)) \sum_{i=1}^M \sum_{j=1}^N f(i, j)$, meanwhile, to determinate the standard deviation (σ) also the approach for a 2D sample is used $\sigma = \sqrt{\left(\frac{1}{M \times N}\right) \sum_{i=1}^M \sum_{j=1}^N (f(i, j) - \mu)^2}$. The area of the segmented regions using a threshold function can be easily measured since a binary image is obtained.

Edge Detection

An edge is one of the most natural and simple ways to recognize objects in a scene or picture for human beings; for computers, the gradient approach aims at finding strong local intensity changes that denote the existence of an edge.²⁰ Roberts cross operator is a simple approach to the continuous gradient at the interpolated point not to the point itself. It first estimates the horizontal, G_x , and vertical edges, G_y , individually and then merges the results.²¹ G_x is the kernel mask $\begin{bmatrix} 1 & 0 \\ 0 & -1 \end{bmatrix}$, meanwhile G_x is formulated as $\begin{bmatrix} 0 & 1 \\ -1 & 0 \end{bmatrix}$. On the other hand, the Prewitt operator is the magnitude of the gradient, P , about the interpolated point using the information of the 3×3 neighborhood. The horizontal gradient, P_x , and the vertical gradient, P_y , that are estimated using kernel masks of 3×3 with the left column and the superior row with -1 values, meanwhile the right column and the inferior row have $+1$ values, finally, the central column and row are filled

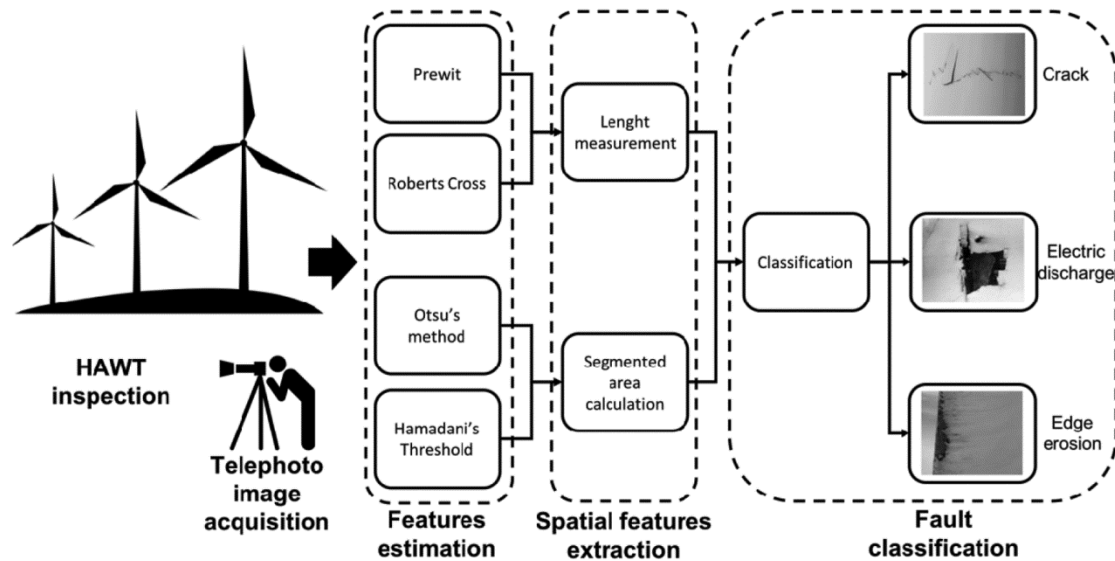


Fig. 1 — Proposed wind turbines blade damage classification, HAWT and photographer images by Abdul Karim and Luis Prado from the Noun Project respectively

with zero values respectively. Because of this, Prewitt gradient gives same emphasizes to the pixels of the kernels as opposition to the Sobel gradient that emphasis central pixels.²² Edge detection allows obtaining geometric measures of the segmented objects like length, width, and perimeter.

Wind Turbines Blades Damage Classification

For this work, the methodology shown in Fig. 1 is used. It starts with the proposal of a HAWT inspection which is performed at ground level. This inspection is based on the use of a reflex camera with a telephoto mounted on a tripod. The reflex camera has the following specifications: Nikon D5300, CMOS sensor, 24.4 megapixels image, Wi-Fi integrated and GPS; meanwhile, the telephoto lens used is the SIGMA 70–200 mm $f/2.8$. The image acquisition is performed by the user from the root end to the tip of each blade, front and backward and for each one of the blades following its numbering (1, 2 and 3) as is printed on them. After the images are acquired, they are transferred by wireless to a PC with the automatic analysis system installed. Since every image is georeferenced this parameter allows to the user to organize every image set per air turbine. Next, a region of interest (ROI) selection is performed manually by the user to focus on the specific problems detected for every image. Multiple ROI can be selected by the user in the case of multiple problems observed. Finally, the analysis process starts. The cropped image is first processed to make the features estimation. These features are

Table 1 — Features analyzed qualitatively

Fault type	Qualitative evaluation
Crack	<ul style="list-style-type: none"> - Thin lines - Small areas of segmented objects - Large segmented lines
Electric discharge	<ul style="list-style-type: none"> - One big object area - Proportional height and width lengths
Edge erosion	<ul style="list-style-type: none"> - One big object area - Significate difference of length and width size

remarked using automatic threshold algorithms and edge detectors. Each image is processed with the four algorithms presented in the previous section in parallel. This is done just in the case that certain algorithm does not detect anything, so the other algorithms are backing up the process. Once the features are enhanced they are measured in the following step. Length and area are registered using pixels as measuring unit. And from there a classification process is performed to determinate the type of fail registered: crack, electric discharge or edge erosion. The user receives, as result, an image processed with the fail segmented and the result of the classification.

Results and Discussion

As an initial step, prior to starting the classification of faults in turbine images, a qualitative extraction of features was manually performed. The images were processed using the automatic thresholds and edge detectors. Then a user evaluated the image features. Table 1 resumes the results of this initial process; it

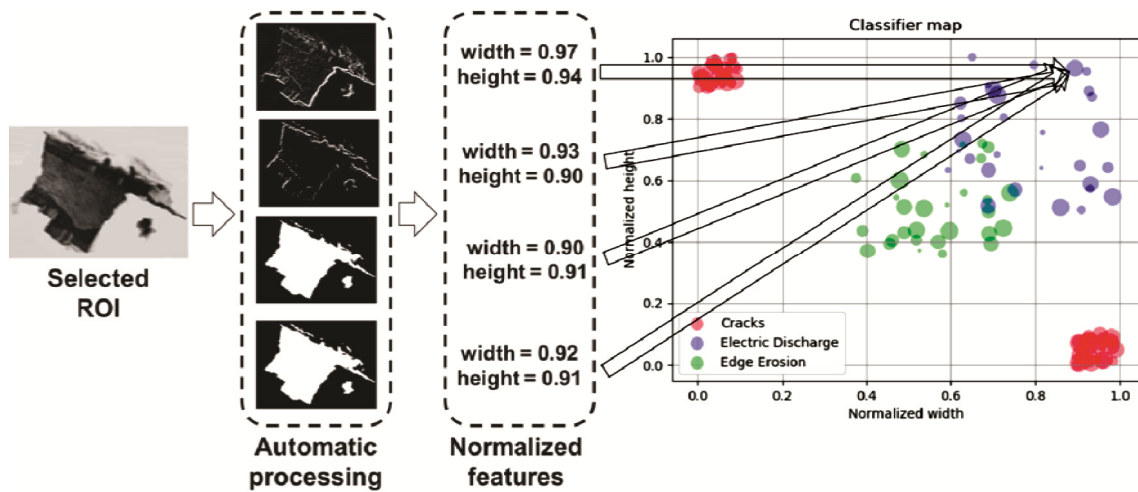


Fig. 2 — Fault classification process

was possible to see that cracks generally are segmented into thin and large lines therefore, their areas tend to be small; electric discharge, meanwhile, it presents one big object segmented, such object is proportional to its height in relation to its width; and finally border edge erosion also is segmented as one big object, however this time the object tends to be larger.

The tests of the classifier were conducted using synthetic and real images acquired in some Eolic parks installed in La Ventosa, Oaxaca, Mexico; it is important to mention that maintenance information and images are reserved as part of the industrial secret, and in general the companies does not allows to perform tests or take images on their wind turbines, besides they do not provide access to real inspection reports. In the case of the acquired images, it is not possible to display or share them due to confidentiality agreements. In Fig. 2, a concept image to visualize the evaluation and classification based on the length and width process is shown. The acquired images are processed to estimate and measure their features. These are used to determine to which class (1, 2 or 3) the processed image has more probability to belong. Class 1 belongs to cracks and is shown in Fig. 2 denoted with red circles, it is closer to the maximum value of the normalized height with a small normalized width, but also it is closer to the maximum normalized width and small height which is symmetric or a complementary behavior. Class 2, that indicates electric discharge, is indicated in Fig. 2 with blue circles. Such fault is visible to have a proportional height and width, this behavior makes the Class 2 being located in the top right of the classification map. Class 3, denoted in green circles,

has a similar behavior as Class 2 and is one of the most difficult to analyze, however in most of the cases it is possible to differentiate it looking for a significant difference between the length and the width of about 15 to 20%. The successful classification ratio for cracks in wind turbine blades was 90%. Main issues were related to noise in images and completely delete of regions in the features estimation process caused by cracks barely visible in the images. Efficiency classification of erosion in the border edge and electric discharge was 80% due to a high similitude between them. Main issues were related to incorrect ROI selection and perspective errors. Besides, some border edge problems also present a regular proportion between width and height which overlaps Classes 2 and 3.

Conclusions

In this paper, a new methodology that aims to provide an automatic classification of faults in wind turbine blades inspection using image processing was presented. The proposed method to acquire the images is very similar to the standard inspection method using a telescope, the addition of a telephoto mounted in a reflex camera allows to immediately register any detected problem. Geotagging of the images, on the other hand, provides valuable information that can help to establish damages behaviors in certain zones of the Eolic parks due to, i.e., manufacturing problems of the turbine blades or incorrect maintenance operations. Regarding the images treatment, basic image processing algorithms can be enough to enhance features in the acquired images, however additional algorithms should be

included in the future to get a wider range of parameters to include in the faults classifier, allowing to discriminate even more types of problems. The presented automatic classifier algorithm can provide a valuable supportive tool in the inspection procedures reducing times in the decisions making.

Acknowledgements

This work was partially supported by project SEP-CONACyT 222453-2013.

References

- Blaji G & Gnanambal I, Wind power generator using horizontal axis wind turbine with convergent nozzle, *J Sci Ind Res*, **73** (2014) 375–380.
- Fried L, Shukla S, & Sawyer S, *Growth Trends and the Future of Wind Energy*, (Elsevier), (2017), 559–586
- Sovacool BK, Contestation, contingency, and justice in the Nordic low-carbon energy transition, *Energy Policy*, **102** (2017) 569–582
- Hau E, Physical Principles of Wind Energy Conversion, In: *Wind Turbines*, (Springer Berlin Heidelberg, Berlin, Heidelberg), 2013, 79–87
- Wymore ML, Van Dam JE, Ceylan H, & Qiao D, A survey of health monitoring systems for wind turbines, *Renew Sustain Energy Rev*, **52** (2015) 976–990
- Pan ZJ, Wu JZ, Liu J, & Zhao XH, Fatigue Failure of a Composite Wind Turbine Blade at the Trailing Edge, *Defect Diffus Forum*, **382** (2018) 191–195
- Loh CH, Loh KJ, Yang Y Sen, Hsiung WY, & Huang YT, Vibration-based system identification of wind turbine system, *Struct Control Heal Monit*, **24** (3) (2017) 1–19
- Willis DJ, Niezrecki C, Kuchma D, Hines E & Arwade S, Wind Energy Research: State of the Art and Future Research Directions, *Renew Energy*, (2018)
- Sarrafi A, Mao Z, Niezrecki C, & Poozesh P, Vibration-based damage detection in wind turbine blades using Phase-based Motion Estimation and motion magnification, *J Sound Vib*, **421** (2018) 300–318
- Li X, Sun J, Tao N, Feng L & Shen J, An Effective Method to Inspect Adhesive Quality of Wind Turbine Blades Using Transmission Thermography, *J Nondestruct Eval*, **37** (2) (2018) 19
- Tchakoua P, Wamkeue R, Ouhrouche M, Slaoui-Hasnaoui F & Tameghe TA, Wind turbine condition monitoring: State of the art review, new trends, and future challenges, *Energies*, **7** (4) (2014) 2595–2630
- Gómez Muñoz CQ, García Márquez FP, & Sánchez Tomás JM, Ice detection using thermal infrared radiometry on wind turbine blades, *Meas J Int Meas Confed*, **93** (2016) 157–163
- Galleguillos C, Zorrilla A, Jimenez A, Diaz L & Montiano ÁL, Thermographic non-destructive inspection of wind turbine blades using unmanned aerial systems, *Plast Rubber Compos*, **44** (3) (2015) 98–103
- Głowacz A & Glowacz Z, Diagnosis of the three-phase induction motor using thermal imaging, *Infrared Phys Technol*, **81** (2017) 7–16
- Jain S, Jagtap V, & Pise N, Computer aided melanoma skin cancer detection using image processing, in *Proc Comput Sci*, **48** (Elsevier), 2015, 736–741
- Garduño-Ramón MA, Vega-Mancilla SG, Morales-Hernández LA, & Osornio-Rios RA, Supportive noninvasive tool for the diagnosis of breast cancer using a thermographic camera as sensor, *Sensors (Switzerland)*, **17** (3) (2017) 1–21
- Resendiz-Ochoa E, Osornio-Rios RA, Benitez-Rangel JP, Morales-Hernandez LA, & Romero-Troncoso RJ, Segmentation in thermography images for bearing defect analysis in induction motors, *Diagnostics Electr Mach Power Electron Drives (SDEMPED)*, 2017 IEEE 11th Int Symp, (Im) (2017) 572–577
- Elbayoumi Harb SM, Isa NAM, & Salamah SA, Improved image magnification algorithm based on Otsu thresholding, *Comput Electr Eng*, **46** (2015) 338–355
- Gao B, Li X, Woo WL, & Tian G yun, Physics-Based Image Segmentation Using First Order Statistical Properties and Genetic Algorithm for Inductive Thermography Imaging, *IEEE Trans Image Process*, **27** (5) (2018) 2160–2175
- Burger W & Burge MJ, *Digital Image Processing*, (Springer London, London), (2016), 811
- Chen X, Wang S, Zhang B, & Luo L, Multi-feature fusion tree trunk detection and orchard mobile robot localization using camera/ultrasonic sensors, *Comput Electron Agric*, **147** (2018) 91–108
- Razmi M, Asgari HM, Sohrab AD, Mohammad S & Nazemosadat J, Monitoring oscillations coastline of Dayyer city during the El Niño and La Niño using OIF utility index, *Indian J Geo Mar Sci*, **46** (11) (2017) 2286–2289